2D-LIF Investigation of the Early Stages of Flame Kernel Development during Spark Ignition

J.Xu, F.Behrendt and J.Warnatz
Institut für Technische Verbrennung
Universität Stuttgart
Pfaffenwaldring 12, D-70569, Stuttgart
Germany

ABSTRACT

Spark ignition of methanol-air mixtures in a combustion chamber at different spark gap widths have been studied using two-dimensional laser-induced fluorescence imaging of OH radicals. The Q13 line of hydroxyl in the (0.0) vibrational band of the $A^2\Sigma$ - $X^2\pi$ transition was excited by a frequency-doubled dye laser, which is pumped by a XeCl excimer laser. 2D-LIF images of OH radicals from a cross-section through the ignition kernel have been obtained during the ignition process. Two fundamental spark kernel structures, spherical and toroidal, are seen clearly in these images. It is found that the formation of toroidal structure depends on the spark gap width. Larger gap widths benefit the formation of toroidal structure.

INTRODUCTION

Spark ignition is the first step in spark ignition engines, which strongly affects the overall combustion process in engines [1, 2]. A detailed understanding of the spark ignition process is important to designing engines, improving fuel economy, and reducing pollutant emission.

For a better understanding of this process, much experimental work has been done with schlieren, shadowgraph, and interferometer techniques [3, 4]. The results lead to the conclusion that the development of a spark kernel and the propagation of a flame in the combustible mixtures can be studied with these techniques, but due to the integrating nature of schlieren and interferometric techniques drawing firm conclusions about the chemical structure of the flame kernel is very difficult. Laser-based techniques offer the capability for spatially and temporally resolved measurements of important chemical parameters.

Two-dimensional laser-induced fluorescence (2D-LIF) is one of the most useful laser spectroscopic probes which has been developed and successfully applied to combustion research over the past several years [5]. In this technique, a laser beam is transformed by cylindrical lenses into a light sheet, which intersects the flow field in a plane. Laser excited particles are observed by a two-dimensional detector such as a CCD camera.

The OH molecule has been the most commonly studied combustion species using LIF because of its relative abundance in combustion process and the availability of convenient UV laser systems to excite the $A^2\Sigma$ - $X^2\pi$ electronic transition. The spectroscopic parameters describing this transition are well known. OH radicals are formed by several reactions in the flame front, such as the principal chain-branching process $H + O_2 = OH + O$ [6], in addition, it is also present in the burnt gases according to its thermal equilibrium concentration. Thus, OH marks the regions where the combustion is taking place and has already taken place .

In this paper, 2D-LIF images of OH radicals from a cross-section through the ignition kernel have been obtained during the ignition process. The temporal and spatial structure of the ignition kernel has been observed at different spark gap widths. In comparision to conventional experimental techniques used by other researchers, 2D-LIF imaging provides a clearer picture of the development of the spark igntion kernel.

EXPERIMENTAL SET-UP

The experimental system for 2D-LIF of OH radicals in the ignition kernel has been described in detail in previous work [7]. For completeness the description is partly repeated. This experimental set-up is schematically illustrated in Fig. 1. It consists of an ignition system, a combustion chamber, a laser, and a LIF detection system.

Spark discharges are generated by an ignition system which consists of a capacitance spark circuit and a dc discharge supply system. The capacitance spark circuit produces a weak breakdown discharge (0.1 mJ) of short duration (1 μs). This breakdown discharge provides a conductive channel between the electrodes for the following dc discharge. The duration of dc discharge can be varied from 10 μs to 300 μs, its power is 37 W.

The constant volume combustion chamber (150 mm diameter and 160 mm height) contains orthogonal sets of UV-transmitting quartz windows with 40 mm diameter, providing optical access for observation of the combustion process. A pair of copper wires (0.4 mm diameter) with blunt ends is used as electrodes. The spark gap is located at the centre of the chamber.

Experiments are performed using methanol-air mixtures. The gas mixture ratios are determined by the method of partial pressures. The pressure gauge is an analog electronic pressure transducer coupled to a digital voltmeter (MKS Type 122A) with an accuracy of 0.5%. In order to ensure complete mixing of methanol and air inside the combustion chamber, one should

wait at least ten minutes before combustion is initiated.

The UV laser light for the fluorescence excitation of the OH radicals is provided by a tunable dye laser system (Lambda Physik FL3002E, Rhodamine B dye) with frequency doubling using a KDP crystal. The dye laser is pumped by a XeCl excimer laser (Lambda Physik LPX 200). The laser pulse from the dye laser was tuned at 308.154 nm to pump the Q13 Line in the (0.0) vibrational band of the $A^2\Sigma - X^2\pi$ transition. The duration and the energy of the laser pulse are 20 ns and 1 mJ. The laser beam is formed by lenses into a light sheet of 12 mm height and 0.1 mm thickness and passes through the centre of the combustion chamber with about 0.3 mm clearance from the axis of the electrodes. Fluorescence radiation from OH radicals is collected at a right angle to the laser sheet by a CCD camera (Proxitronic Nanocam) with UV objective (Nikon 1/4.5, f = 105) and image intensifiers. A UV transmission filter UG5 is located in front of camera to reject the luminescence of the flame. The camera signal is digitized by a frame grabber board inside a PC. The ignition system, the laser system, and the CCD camera are triggered by a delay pulse generator with appointed delay times. Therefore, the map of OH radicals can be obtained at any time during spark ignition process.

RESULTS AND DISCUSSION

Measurements of Initial Shock Wave:

A conventional laser-schlieren photography is used to measure the initial shock wave induced by the breakdown discharge. These experiments have been carried out in the combustion chamber using air at atmospheric pressure, with different spark energies and different electrode distances. It has been found that the strength of the initial shock wave depends mainly on the energy of the breakdown discharge [3, 8]. In this case, a measurement of the energy of breakdown discharge produced by this ignition system is necessary.

The ignition energy from the breakdown phase can be calculated from $E_b = 0.5 \cdot C \cdot V_b^2$, where C is the capacitance of the electrodes (measured to 2.4 pF), and V_b the breakdown voltage. The measured breakdown voltage and the calculated energy of the breakdown discharge as a function of gap width are presented in Fig 2. It can be seen that the breakdown voltage increases with increasing gap width. The energy of breakdown discharge is directly proportional to the gap width. This result corresponds with results of Ziegler et al. [9]. So, the ratio of energy E_b of breakdown discharge and electrode distance d is constant, when the capacitance of the spark circuit is kept constant.

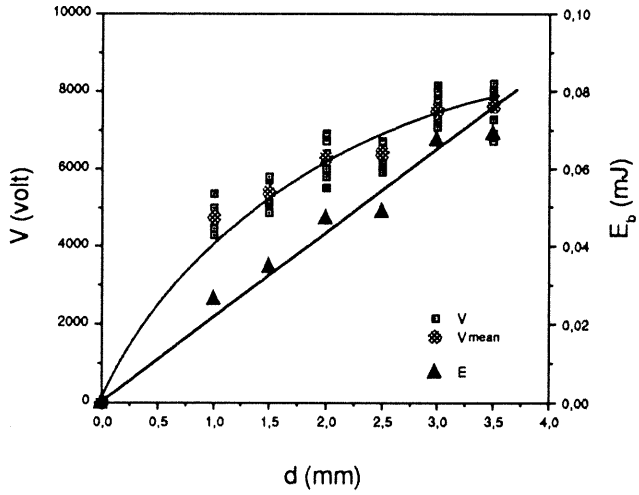

Fig 2. The measured breakdown voltage V and the calculated energy of the breakdown discharge E as functions of gap width

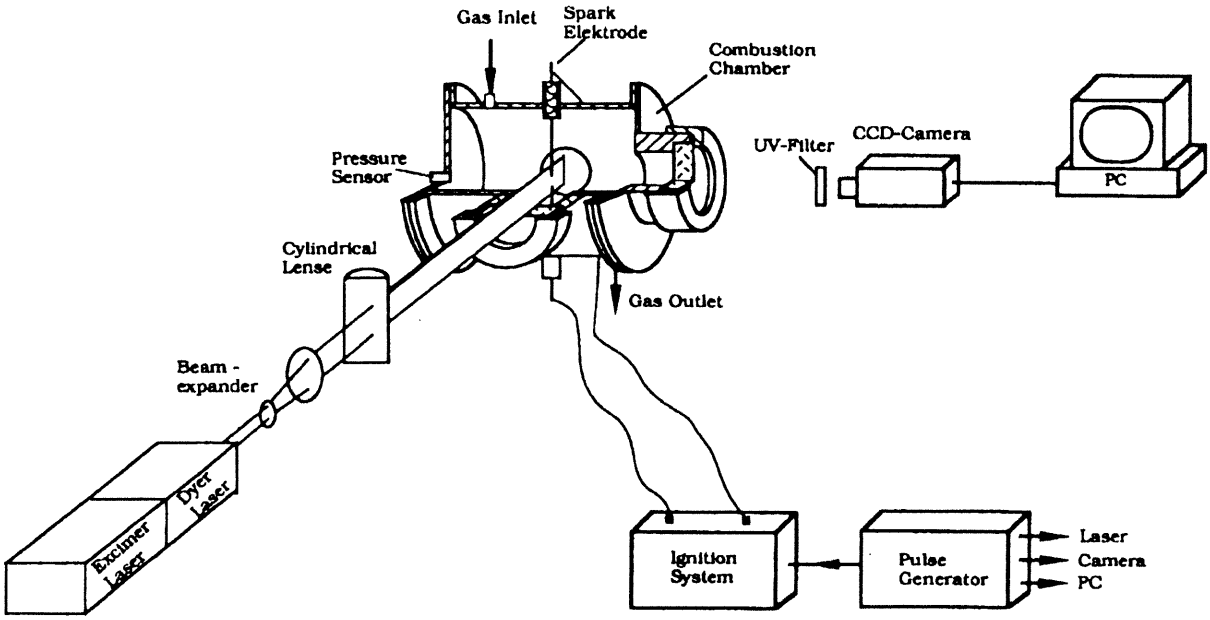

Fig. 1 Experimental set-up of 2 - D LIF imaging experiment of spark ignition

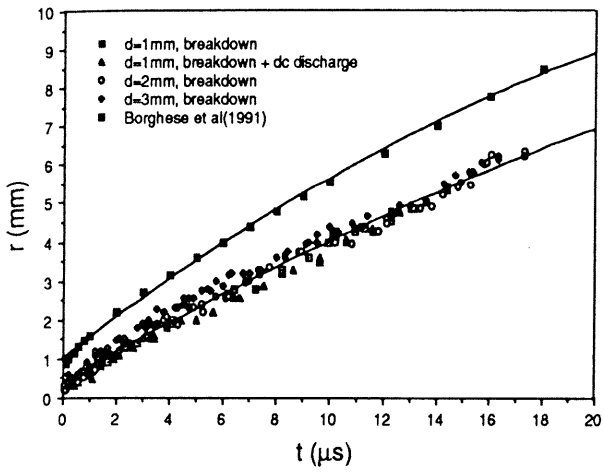

Fig. 3 Radius of shock wave front r as a function of time t during the initial shock wave propagation

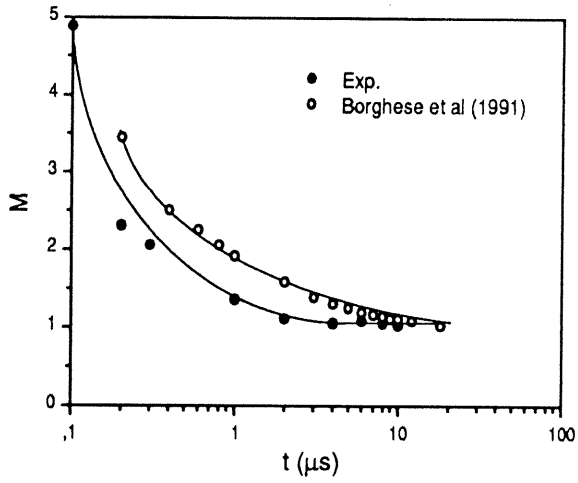

Fig. 4 Mach number M of shock wave versus time t during the initial shock wave propagation

Laser-schlieren photographs show that the initial shock wave induced by the breakdown discharge separates from the very hot discharge channel at about 1 ms and travels into surrounding atmosphere in a spherical shape. The position of the shock wave front r at different time during the shock wave propagation is plotted in Fig. 3. In addition, results of Borghese et al. [8] (spark energy = 14 mJ, duration = 100 ns, gap width = 2 mm) are plotted in this figure for comparison.

It can be seen that traces of shock wave fronts obtained in this work can been fitted with a single curve. Because the discharge channel is quickly heated to 60 000 K during the breakdown discharge [3,4], the pressure therein increases immediately to several hundred bar [4]. The discharge channel expands during this period with supersonic speed causing the initial shock wave. The expansion of the discharge channel is determined by the temperature and pressure within the channel, which, in turn, depend only on E_b/d. So, the propagation speed of the shock wave is determined by the ratio of E_b and d. In this work, the capacitance of the spark circuit is kept constant resulting in a constant E_b/d (see Fig. 2). Therefore, at different spark width gaps the propagating speed of the shock wave remains the same.

Exploiting the data of Fig. 3, the speed of the shock wave versus time is given in Fig. 4. As shown in Fig. 4, the speed of the initial shock wave decreases very fast. At about 20 μs the Mach number of the shock wave of this work is close to unity, and the shock wave transforms into a sound wave. The area disturbed by the initial shock wave has a radius of about 6 mm.

Measurements of Methanol Ignition Limits:

Ignition limits of methanol-air mixtures at different pressures were measured. The initial temperature of the mixtures is 296 K. The minimum ignition energy of a combustible mixture is determined as follows: For a given combustible methanol-air mixture and spark energy, the discharge is repeated ten times. If the mixture is not ignited, the spark energy will be increased in small steps (0.16 mJ) until at least one ignition happens in ten successive sparks. This value of spark energy is defined as minimum ignition energy of this mixture.

Fig. 5 shows the ignition limits of methanol-air mixtures

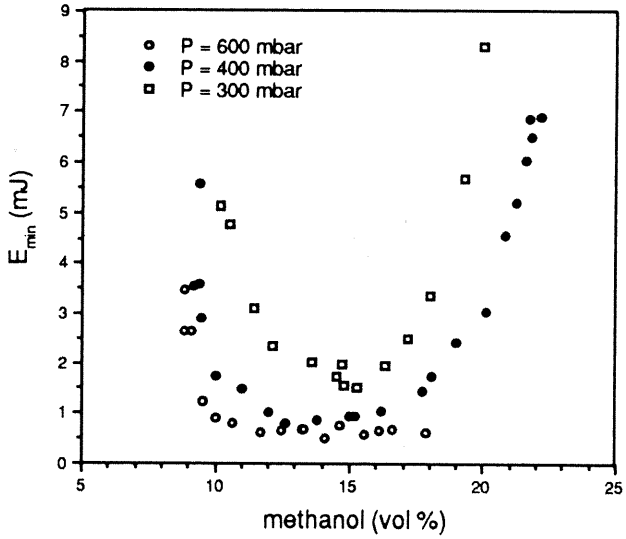

Fig. 5 Ignition limits of methanol-air mixtures at different pressures, spark gap width: 2 mm

at different pressures. One can see that a methanol-air mixture is combustible when the methanol content is between 9 and 22 vol%. The minimum ignition energy is seen to increase with decreasing pressure for a given methanol-air mixture.

2D-LIF Images of Spark Ignition Kernel:

Fig. 6a shows a series of 2D-LIF images of OH radicals from a cross-section through a developing ignition kernel. The ignition kernel is produced by a spark with energy of 1.6 mJ and a duration of 35 μs. Its gap width is 3 mm and the initial pressure is 600 mbar. Each of these images is obtained from a separate experiment by time delaying the excitation laser pulse relatively to the onset of the ignition spark. However, because of the high degree of reproducibility of the phenomenon at the same experimental conditions, the series of images can be considered as a motion picture of a single experiment. In the fluorescence image, a colour-scale scheme is used to show areas of different relative OH concentration, with black representing no OH

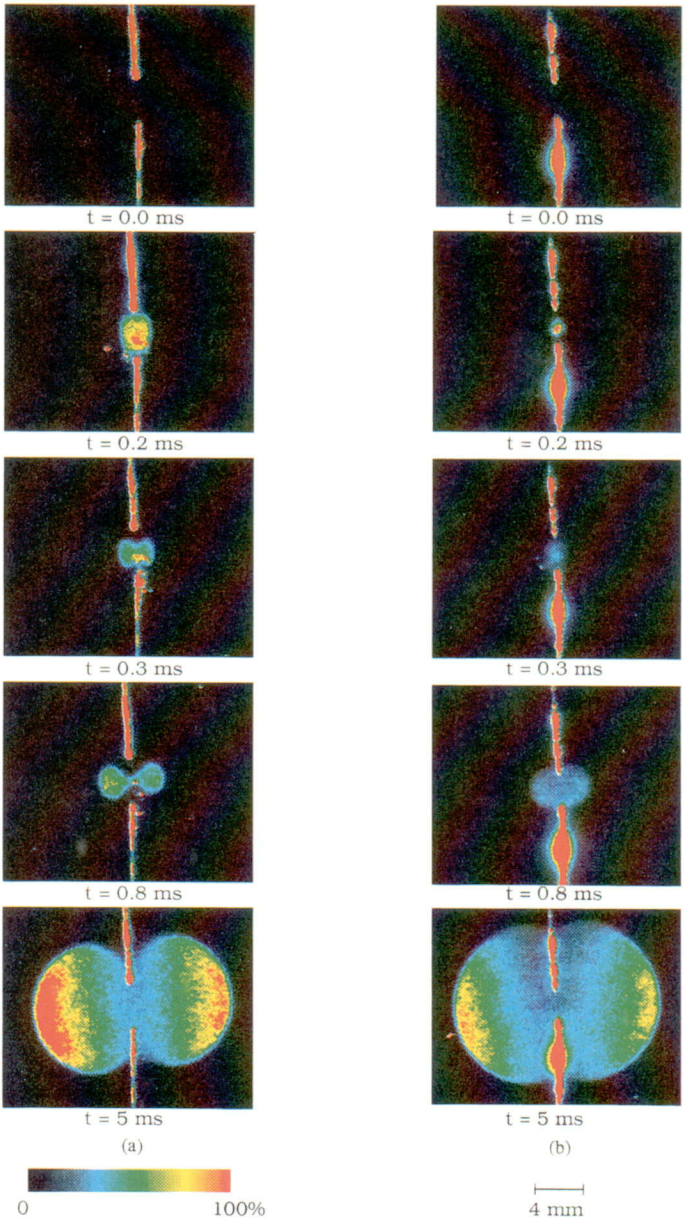

Fig. 6 2D OH - LIF imagings of spark ignition kernel at different times during the ignition of methanol-air mixture, methanol: 11% vol, spark energy = 1.6 mJ, spark duration = 35 µs, pressure = 600 mbar
a) spark gap width = 3 mm; b) spark gap width = 2 mm

radicals, red the highest concentration.

In order to reduce laser obstruction from electrodes, the laser sheet is shifted 0.3 mm out of the axis of electrodes towards the CCD-camera. So, the disturbance of electrodes is very small and also they can be seen by reflected laser light. The signal in the first image of Fig. 6a is only due to reflections of the laser light and marks the positions of electrodes and gap.

The LIF images in Fig. 6a show that at about 0.2 ms after the onset of the spark a reaction zone with high OH concentration is seen between the electrodes. The roughly cylindrical reaction zone is formed by the narrow cylindrical discharge channel which has a high temperature. About 0.3 ms after the onset of the spark, the flame kernel is seen to be compressed around the connecting axis between the electrodes (see LIF image at 0.3 ms in Fig. 6a). This phenomenon is closely related with shock wave behaviour produced by the breakdown phase. At about 1 ms the shock wave separates from the hot discharge channel and travels into the surrounding atmosphere. Inside the shock wave the gas moves outwards with high velocity. The movement of gas causes a slight over-expansion after the shock wave, although it separates rather far from the residual hot kernel. The over-expansion induces an inward gaseous flow along the electrodes surfaces toward the spark gap [8, 10]. This flow distorts the initially formed cylindrical spark kernel into a torus.

If the spark energy is large enough, or in other words, the temperature of the toroidal ignition kernel is high enough, a self-sustained flame will be generated and propagate from the surface of the toroidal ignition kernel into the surrounding combustible mixture, as shown by 2D-LIF images at 0.8 ms and 5.0 ms in Fig. 6a.

At about 5 ms after the onset of the spark, the highest OH concentration area appears near the edge of the ignition kernel, as can be seen from the colour of the corresponding 2D-LIF image. It means that the flame front begins to emerge from the ignition kernel. The OH concentration rises sharply through the flame front to its peak value and then decreases gradually due to slow recombination reactions in the post flame gases. Therefore, the colour of the centre of the ignition kernel in LIF image is not black. Due to the low energy in the initial breakdown, the flame front is not distorted by the gas movement induced by the initial shock wave.

To compare the influence of the spark gap width on the establishment and growth of a spark kernel, a set of experiments has been carried out with a spark gap width of 2 mm. Other conditions were the same as that in experiments described above.

2D-LIF images of the ignition kernel produced by the spark with 2 mm spark gap width are shown in Fig. 6b. In this case, the discharge channel is close to a "point-like" source. Because of heat conduction towards the electrodes, the region near the electrodes is cooled. The initial spherical reaction zone appears in the middle of the spark gap. One can see that the spark ignition kernel remains always spherical. The inward flow caused by the initial shock wave weakly influences the development of the ignition kernel. A toroidal structure does not occur during the spark kernel propagation. So, at small spark gap widths the assumption of a spherical geometry of the spark ignition kernel corresponds well with experimental findings.

CONCLUSIONS

In this work, two-dimensional laser-induced fluorescence imaging of OH radicals has been used to study the spark ignition of methanol-air mixtures. 2D-LIF images of OH radicals from a cross-section through the ignition kernel during the ignition process have been obtained. They provide a clearer picture of the development of spark igntion kernel.

Two fundamental spark kernel structures, spherical and toroidal, have been observed. A toroidal structure of ignition kernel is clearly visible in these images. The formation of the toroidal structure depends on the spark gap width. Larger spark width benefits the formation of toroidal structure.

The inward gas flow induced by the initial shock wave from the breakdown phase has a significant influence on the development of the ignition kernel. The assumption of a spherical geometry of the spark ignition kernel is only applicable to describe the ignition induced by an electrical spark with a small gap width. In order to provide a more realistic description of spark ignition the inward gas flow induced by initial shock wave must be taken into account, which affects the energy and mass transfer between the spark kernel and fresh gas at early times of spark ignition.

REFERENCES

[1] Chomiak, J., Seventeenth Symposium (International) on Combustion, pp. 255 - 263, The Combustion Institute, Pittsburgh (1978).

[2] Maly, R., Saggau, B., Wagner, E., and Ziegler, G.F.W., SAE Paper 830478 (1983).

[3] Meer, J. M., in "Electrical Breakdown of Gases" (J. M. Meek and J. D. Craggs, Eds.), pp. 753 - 838, Wiley, New York (1978).

[4] Maly, R., in "Fuel Economy in Road Vehicles Powered by Spark Ignition Engines" (Hilliard, J. C. and Springer, G.S.), pp. 91 - 148, Plenum Press (1984).

[5] Hanson, R. K., Twenty-First Symposium (International) on Combustion, pp. 1677 - 1691, The Combustion Institute, Pittsburgh (1986).

[6] Warnatz, J., Eighteenth Symposium (International) on Combustion, pp. 369 - 382, The Combustion Institute, Pittsburgh (1981).

[7] Xu, J., Warnatz, J., Ber. Bunsenges. Phys. Chem. 97 pp. 1741 - 1744 (1993).

[8] Borghese, A., D'Alessio, A., Diana, M., Venitozzi, C., Twenty-Second Symposium (International) on Combustion, pp. 1651 - 1659, The Combustion Institute, Pittsburgh (1988).

[9] Ziegler, G.F.W., Wagner, E.P., Maly, R., Twentieth Symposium (International) on Combustion, pp. 1817 - 1824, The Combustion Institute, Pittsburgh (1984).

[10] Kono, M., Niu, K., Tsukamoto, T., and Ujie, Y., Twenty-Second Symposium (International) on Combustion, pp. 1643 - 1649, The Combustion Institute, Pittsburgh (1988).